Romanian Reports in Physics, Vol. 66, No. 4, P. 1029–1037, 2014

HUMAN EYE MAGNETIC RESONANCE IMAGING RELAXOMETRY IN DIABETIC RETINOPATHY

L. FANEA[1], S. NICOARA[2], S.V. BODEA[3], S.A. SFRANGEU[1,4]

[1] Cluj County Emergency Hospital, Radiology Department, 3-5 Clinicilor str, 400006 Cluj-Napoca, Romania
E-mail: laura_fanea@yahoo.com
[2] "Iuliu Hatieganu" Medicine & Pharmacy University, Ophthalmology Department, 3-5 Clinicilor str, 400006 Cluj-Napoca, Romania
[3] Clinic for Diagnostic and Interventional Neuroradiology, Kirrberger str, Building 90, D-66421 Hamburg/Saar, Germany
[4] "Iuliu Hatieganu" Medicine & Pharmacy University, Radiology Department, 3-5, Clinicilor str, 400006 Cluj-Napoca, Romania

Received February 20, 2014

Abstract. Two quantitative ocular magnetic resonance imaging (MRI) methods for the clinical use in Ophthalmology and Radiology were developed. Ocular MRI images with spatio-temporal resoultions of 0.78/1.56/2/(5 to 84) mm/mm/mm/s were acquired from patients with diabetic retinopathy and normal subjects using a 1 T MRI system. T_1 and T_2 MRI relaxometry maps were generated offline from the MRI images acquired. Statistically significant differences between the T_1 values of the normal and disease-affected groups were found. Useful qualitative and quantitative ophthalmological, radiological and surgical information covering the whole eye can be achieved using noninvazive MRI techniques.

Key words: MRI, relaxometry, radiology, ophthalmology, diabetic retinopathy.

1. INTRODUCTION

According to statistics in 2008, 347 million people from 199 countries suffer from diabetes [1]. Diabetic retinopathy (DR) is a complication of diabetes mellitus caused by the deterioration of the small blood vessels nourishing the retina which may leak fluid or blood [2] and it is an important cause of blindness [3]. According to the WHO statistics, one percent of global blindness can be attributed to diabetes [4]. Within the group of patients suffering from diabetes mellitus for more than 20 years, more than 75 % will develop some form of DR [3]. Early detection of DR may help preventing the patients' vision loss [3, 5].

Compared to the alternative ocular imaging techniques, magnetic resonance imaging (MRI) can image noninvasively the whole eye, without the need of transparent media, in acquisition times as short as a few seconds with spatial resolution good enough to enable visualization of the main eye structures. Additional to the qualitative information of the human eye anatomy, MRI can also provide quantitative information on the pathophysiology of the human eye through measurements of several fundamental tissue properties [6].

MRI images represent maps of the nuclear magnetic resonance (NMR) signals detected by specially designed radiofrequency receiver antenna. The clinical potential of the NMR technique was demonstrated in the 1970s when it was shown that T_1 and T_2 relaxation times of tumors were significantly different compared to those of the normal tissue [7].

The T_1 relaxation time describes how fast the ^{1}H nuclei in water molecules in the region of interest (ROI) will transmit their surplus of energy to the surrounding tissue [8]. The T_2 relaxation time measures how fast the energetic surplus of the ^{1}H nuclei in water molecules in the ROI is transmitted to the neighbor ^{1}H nuclei in water molecules [9]. The decrease or the increase of one and/or both of these parameters compared to the corresponding values measured in the normal tissue can be used to evaluate quantitatively the pathophysiology [10].

The relaxation time values can also give information on the physical properties of the tissue of interest [11] and can, therefore, be used to detect the presence of hemmorrhages, tumors and/or cellular infiltrates in the normal tissue for example.

T_1 [6, 7] and T_2 [12] values were obtained and T_1 maps [13] of human eyes at 1.5 T [12] and 7 T [13] were generated. The potential of the MRI relaxometry for monitoring ocular disease has not yet been studied and its statistical evaluation is required for its future possible implementation in routine clinical ocular MRI.

Quantitative data in clinical imaging in general and in MRI in particular, would provide useful medical diagnostic information for ophthalmologists, radiologists and vitreo-retinal surgeons. The relaxation time maps and the mean T_1 and T_2 values represent quantitative clinical information that might be used in the future as diagnostic tools in ophthalmology, particularly in evaluating patients suffering from DR, but can also be used as a diagnostic tool in the radiological pathophysiological evaluation of any other anatomical structure.

2. METHODS

Consent from each scanned subject and approval from the local Ethical Committee for the evaluation of the clinical potential of the ocular relaxometry MRI at 1 T in DR were obtained prior to performing MRI. The MRI images of 12 normal and 17 human eyes affected by diabetic retinopathy were acquired using a

1 T MRI system (GE, USA) and a single loop surface coil. A 6 ml test tube filled with distilled water was attached to the surface coil, above the scanned eye.

MRI images of each eye were acquired using the 3D spoiled gradient echo SPGR and the steady state free precession SSFP pulse sequences. Acquisition times of a set of images ranged between 5 s and 84 s for one eye, while the whole MRI imaging protocol per eye was almost 15 minutes. Each scanned person kept the eyes closed and as relaxed as possible during the image acquisition. The spatial resolution of the images was $780 \times 1560 \times 2000$ μm^3.

The MRI images were reformatted, the T_1 and T_2 maps were generated and the statistical measurements of the normal and of the eyes affected by diabetic retinopathy were performed offline using MRIcro, MIPAV and in-house codes developed in Matlab. The DESPOT1 method was used for T_1 mapping [14], while T_2 mapping was achieved using linear fittings of each pixel in the image matrix to the signal intensity equation over time using personal codes written in Matlab. These image processing methods were already tested in a phantom study and are detailed presented [15].

Mean T_1 and T_2 values were calculated using MIPAV in the following regions of each examined eye, for both control and DR group: vitreous humor, lens and aqueous humor (Fig. 1). For each group and each eye region, the mean T_1 and T_2 values and their standard deviations were calculated using Excel program. The mean T_1 and T_2 values of the normal and eyes affected by diabetic retinopathy were statistically compared using a two tailed Student t-test of type 2.

Significance in the T_1 and T_2 differences between the same normal and diabetic eye regions were assessed based on the probability (p) values calculated using the t-test. Differences were considered significant (*) for $0.001 < p < 0.05$.

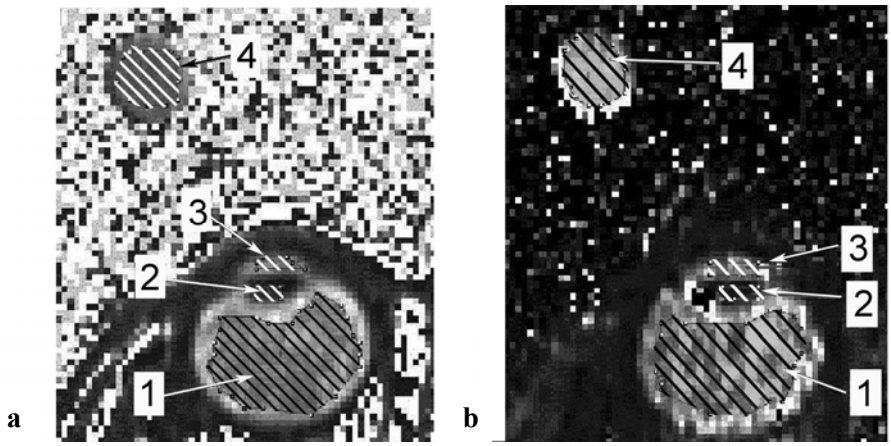

Fig. 1 – Mean values of the T_1 and T_2 values in the regions of the: vitreous humor – 1, lens – 2, aqueous humor – 3 and the phantom – 4, were calculated by drawing the 1 to 4 regions of interest on the T_1: a) and T_2: b) maps.

3. RESULTS

The eye structures visualized using the ocular MRI techniques in this study were: the cornea, the ciliary body, the aqueous humor, the lens, the vitreous humor, the retina/choroid complex, the sclera and the optic nerve. It was possible to perform quantitative measurements only in the vitreous humor, lens and aqueous humor due to the decresed spatial resolution and quality of the MRI relaxometry maps.

A set of MRI sections of a normal left eye and the corresponding T_1 and T_2 maps are presented in Fig. 2.

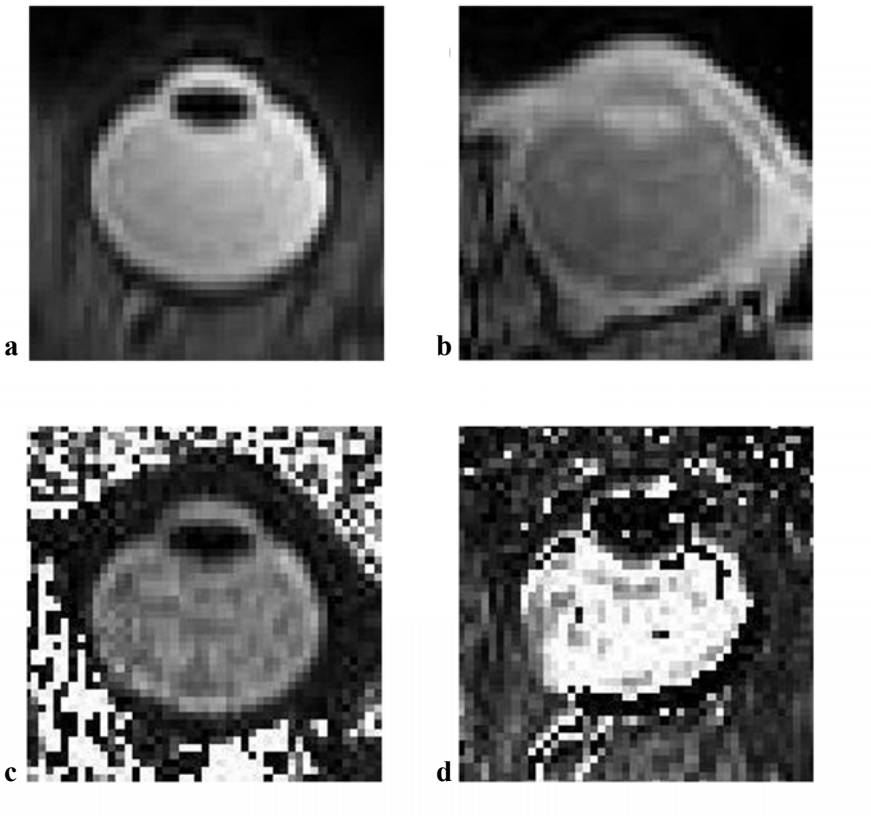

Fig. 2 – Selection of one T_2 – (a) and one T_1 – (b) weighted ocular MRI image used to calculate the T_1 and T_2 maps of the normal human eye shown in: (c) and (d). The signal intensity of the MRI images acquired was linearly fitted using personal written Matlab codes to obtain the T_1 and T_2 maps as described in a previous phantom study [15].

The set of MRI sections with the largest differences in the T_1/T_2 values measured in all the eye structures evaluated compared to the mean T_1/T_2 values measured in the corresponding eye structures of the normal group is presented in Fig. 3. The patient's eye in Fig. 3 was affected by DR and the MRI was performed after pars plana vitrectomy and silicone oil injection. Differences of up to 8.6 times compared to the corresponding control values were calculated in the eye structures evaluated by MRI. These differences were obtained between the mean T_2 values of the normal and DR eyes in the region of the vitreous humor.

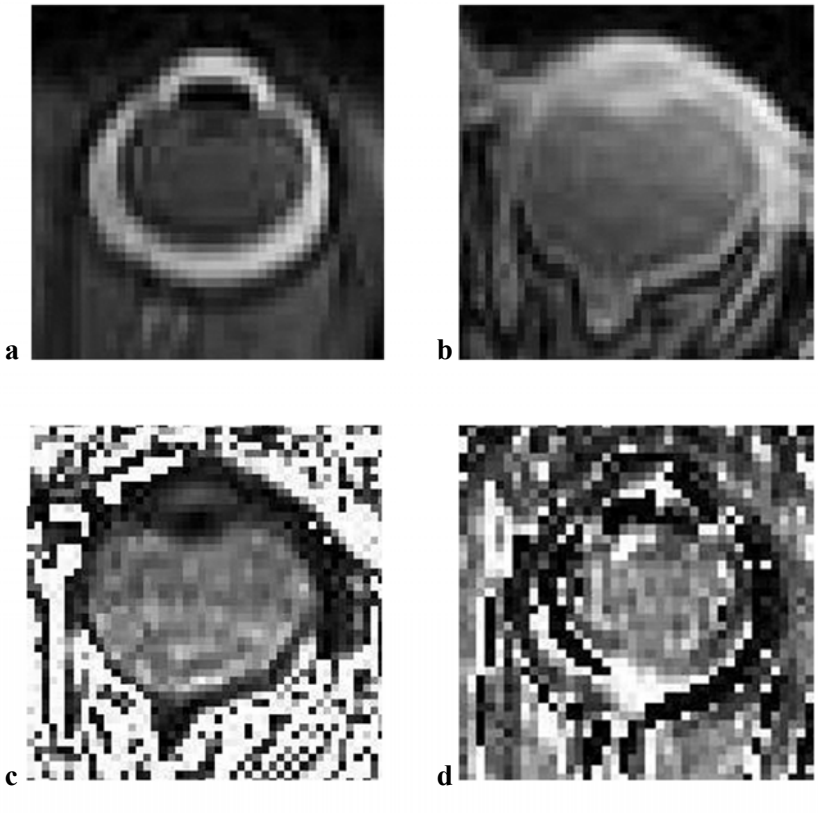

Fig. 3 – The T_2- and T_1- weighted: (a) and (b) ocular MRI images were used to calculate the T_1 and T_2 maps in: (c) and (d). The mean T_1 values calculated on the T_1 map in the region of the vitreous humor/lens/aqueous humor were 4.9 times shorter/4.5 times longer/1.4 times shorter than the corresponding mean T_1 values calculated on the T_1 maps of the normal eyes group. The mean T_2 values calculated on the T_2 map in the region of the vitreous humor/lens/aqueous humor were 8.6 times shorter/1.5 times shorter/1.3 times longer than the mean corresponding T_2 values calculated on the T_2 maps of the normal eyes group.

A comparison of the mean T_1 and T_2 values calculated in different eye structures of the normal human eye at different magnetic field strengths is presented in Table 1. The mean T_1 and T_2 values calculated in the present study in the aqueous humor were approximately the same with those calculated by Patz *et al.* [6] at 1.5 T and 19 % shorter than the mean value calculated by Richdale *et al.* [13] at 7 T. These values are comparatively presented in Table 1. In the region of the lens, the T_1 values were 3.8 and 5 times shorter than those calculated in the corresponding region at 1.5 T [12] and at 7 T [13] respectively. The mean T_2 value in the region of the lens calculated at 1 T in this study was 3.3 times shorter than that calculated in the corresponding ocular region at 1.5 T [12]. The mean T_1 values calculated at 1 T in the region of the vitreous humor were approximately the same with those calculated at 1.5 T [12] and at 7 T [13] but the mean T_2 value was 1.8 times shorter than the corresponding value calculated at 1.5 T [12].

Table 1

Mean relaxation times in different eye structures of the normal human eye. Mean T_1 and T_2 values calculated in different eye structures of the normal human eye at 1 T, 1.5 T [12] and 7 T [13] are compared

Relevant Details for Each Study						
Magnetic Field Strength		1 T	1.5 T [12]	7 T [13]	1 T	1.5 T [12]
Number of Eyes		10	4	4	4: aqueous humor 7: lens 10: vitreous humor	4
Relaxation Times		**T_1 (ms)**			**T_2 (ms)**	
Ocular Region	aqueous humor	5015	5053	6170	439	468
	lens	303	1138	1520	86	26
	vitreous humor	4908	4855	5000	1348	756

At 1 T, statistically significant differences were assessed between the mean T_1 values of the two groups: disease and normal, in the region of the lens and aqueous humor (Fig. 4). No other statistically significant difference between the two groups was found (Figure 4). T_1/T_2 values up to 4.9/8.6 times shorter/shorter than the corresponding mean T_1/T_2 values calculated for the control group was identified. However, most of the values measured in the disease group did not differ significantly compared to the corresponding mean values of the control group. Additional to this, for the same region evaluated in the disease group, the T_1/T_2 values were up to 10/22 % longer in a few eyes, while in other eyes, these were up to 79/88 % shorter compared to the mean values of the normal eyes.

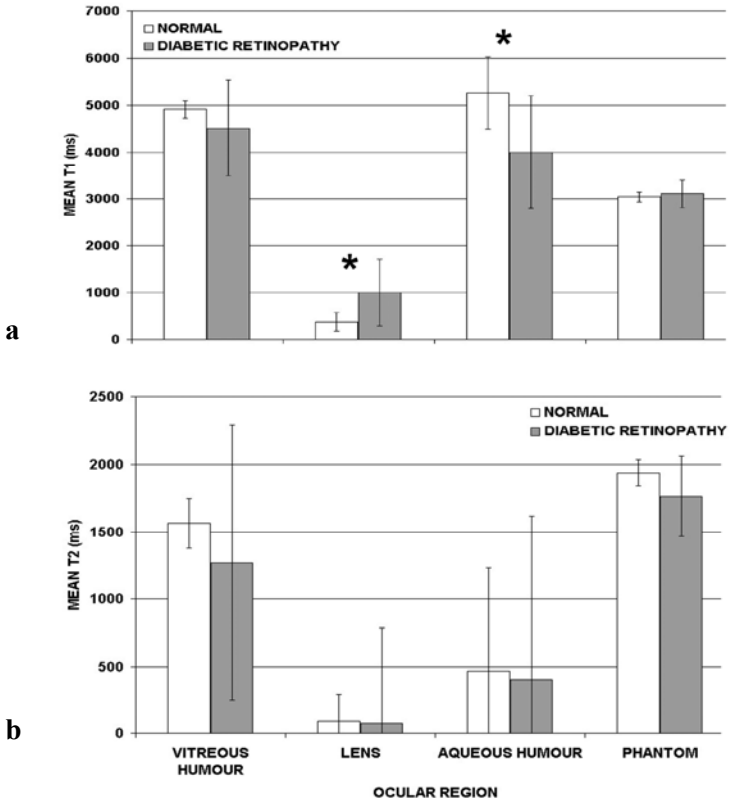

Fig. 4 – The mean T_1 (a) and T_2 (b) values and their standard deviations were calculated for the normal and for the diseased groups. The mean T_1 values (a) calculated for the control and diseased groups were significantly different: $p = 0.005/0.003$, in the region of the lens/aqueous humor. No statistically significant differences were assessed between the mean T_2 (b) values calculated for the control and diseased groups.

4. DISCUSSION

The quantitative information on the mean T_1 and T_2 values of the normal human eye structures at different magnetic field strengths [12, 13] is difficult to analyze due to the different MRI acquisition protocols and/or the post-processing methods used for the extraction of the relaxation times, the different spatio-temporal resolutions of the MRI images or the low number of scanned subjects. It would have been extremely important to have at least a standard value to compare for each of these studies in order to make a realistic comparison of the values calculated for the same ocular structure of the normal human eye at different magnetic field strengths. The comparison of the data can be made referring to T_1

and T_2 relaxation times for a 90 % physiological saline. In this way the T_1 and T_2 calculated values can be normalized to that of the standard phantom. Standardization can be achieved using an adequate phantom as described in this study. In the present study, the mean T_1 and T_2 values in three different structures of the normal human eye and in the eye affected by DR were statistically compared. Significant differences were identified between the corresponding mean T_1 times measured in the lens and in the aqueous humor of the disease and normal group. These are presented with stars in Fig. 4a.

The dispertion of the T_1 and T_2 values in the ocular structures was at least two times larger than in the phantom, with the largest effect seen in the case of the disease group. DR generates many changes in the whole or in small regions of the eye which may affect the physical properties of that region quantified by the relaxation time value measured. To reduce dispersivity of the relaxation times measured in the normal eye structures and in the phantom, the spatio-temporal resolution and the quality of the MRI images need to be improved. This may be achieved by acquisition of the ocular MRI images at higher magnetic field strengths using more performant equipment.

This pilot study analyzed the potential of the ocular MRI relaxometry to quantitatively assess the pathophysiology in general and the ocular pathophysiology in particular. A larger number of subjects, and their division in more refined groups based on the severity of the disease, may lead to more clinically relevant results and would demonstrate the need for the implementation of quantitative MRI imaging methods, including MRI relaxometry, into routine clinical practice.

The T_2 maps of the normal and diseased human eyes were presented in this study together with a statistical analysis of T_1 and T_2 measurements performed in several eye structures for the evaluation of the pathophysiological changes in the eyes affected by DR. The significant differences between the relaxation times of the normal and disease affected eyes can be physiologically correlated with the presence of cellular infiltrates, hemorrhage, silicone in the eye structure evaluated or with the eye structure being affected by cataract. Useful quantitative clinical information covering the whole human eye can be achieved in less than 15 minutes using MRI investigations without contrast agents. More detailed investigations performed on refined groups of normal eyes might be used to realize normative T_1 and T_2 values of the normal eye structures. These values can then be used by radiologists, ophthalmologists but also by surgeons for normal standardization in the future. In conclusion, this study demonstrates that ocular MRI relaxometry at 1 T, performed without contrast agents, brings useful additional quantitative information for the diagnosis, staging and evaluation of ocular disease mechanisms.

Acknowlegments. The first author acknowledges the financial support received from the EC grant POSDRU/89/1.5/S/60189. The authors would like to thank the MRI Radiographers and the healthy volunteers involved in this study.

REFERENCES

1. G Danaei, MM Finucane, Y Lu *et al.*, Lancet, **378**, 31–40 (2011).
2. G Kalantzis, M Angelou, E Poulakou-Rebelakou, Hormones, **5**, 72-75 (2006).
3. Word Health Organization, Available online at: http://whqlibdoc.who.int/publications/2006/924154712X_eng.pdf (2005).
4. World Health Organization, Global data on visual impairments 2010 (2012).
5. E Prokofyeva, E Zrenner, Ophthalmic Res, **47**, 171–188, (2012).
6. L Fanea, AJ Fagan, Mol Vis, **18**, 2538–2560 (2012).
7. CL Partain, J Magn Reson Imaging, **19**, 515–526 (2004).
8. PT Callaghan, *Principles of Nuclear Magnetic Resonance Microscopy*, Oxford University Press Inc, New York, pp. 38–39, (1991).
9. EM Haacke, RW Brown, MR Thompson, R Venkatesan, *Magnetic Resonance Imaging: Physical principles and sequence design*, John Wiley & Sons, New York, 1999.
10. LM Eastwood, JMS Hutchison, JAO Besson, Br J Psychiatry, **146**, 26–31 (1985).
11. MA Foster and A Haase, Encyclopedia of Nuclear Magnetic Resonance, 4034–4040 (1996).
12. S Patz, RJ Bert, E Frederick, et al, J Magn Reson Imaging, **26**, 510–518 (2007).
13. K Richdale, P Wassenaar, KT Bluestein *et al.*, J Magn Reson Imaging, **30**, 924–932 (2009).
14. SCL Deoni, TM Peters, BK Rutt, Magn Reson Med, **53**, 237–241 (2005).
15. L. Fanea, S.A. Sfrangeu, Rom. Rep. Phys., **63**, 456–464 (2011).